JOURNAL OF MATERIALS SCIENCE 30 (1995) 5808–5812

The gravitational effects on low solid-volume fraction liquid-phase sintering

D. F. HEANEY, R. M. GERMAN
P/M Lab, 118 Research West, The Pennsylvania State University, University Park, PA 16802, USA

IN SHUP AHN
Gyeong Sang National University, Chinju, Korea

The gravity effects on liquid-phase sintering (LPS) were experimentally examined by varying the solid- and liquid-phase density difference from 0–9 g cm^{-3}. The overall solid-volume fraction was held at 0.30 to allow free settling of solid grains in the liquid matrix. The solid grains were found to settle and pack to form a solid skeleton with a volume fraction of solid that reflects the density difference.

1. Introduction

Liquid-phase sintering (LPS) is susceptible to a solid–liquid segregation problem due to gravity [1–8]. This segregation phenomenon is related to the density difference between the solid and liquid phases and leads to non-uniform sintered properties due to grain size, grain shape, and solid-volume fraction dependence on vertical position [2–5].

Niemi and Courtney [6] were the first to document quantitatively this solid–liquid segregation phenomenon. They proposed that a solid skeleton forms and prevents further settling when a critical solid-volume fraction is reached. They found the critical solid-volume fraction to be 0.2 for an Fe–Cu system and proposed this to be system-independent because the skeleton structure was thought to be dictated by morphological considerations. Their conclusion of a system-independent solid-volume fraction was later challenged by a study performed by Yang and German [4]. These authors found the critical solid-volume fraction to be 0.60 for a W–Ni–Fe heavy alloy. The Fe–Cu system of Niemi and Courtney's study has a relatively small critical solid-volume fraction and solid–liquid density difference while the W–Ni–Fe system of Yang and German's study has a relatively large critical solid-volume fraction and solid–liquid density difference. These trends indicate that the density difference may affect the critical solid-volume fraction and the resulting microstructure.

The objective of this research was to determine how the segregated solid-volume fraction is related to the solid–liquid density difference. The density difference is believed to influence grain growth and grain interaction which alters the microstructure. Several alloy systems with various solid–liquid density differences were selected for comparison. Comparisons of the height of the segregated region and comparisons of the solid-volume fraction at different vertical positions were made to understand better the processing limits in gravity and the benefits of microgravity processing on low solid-volume fraction LPS systems. These experiments have shown that the settled solid-volume fraction is dictated by the formation of a solid skeleton and can be directly related to the density difference between the solid and the liquid phases. If the density difference is sufficiently large, then solid grains pack to a volume fraction similar to that of maximum loose packing of monosized spheres. When the density difference is small, the falling grain's terminal velocity is lower which allows time for sinter bonds to form a skeleton at a lower packing density.

2. Experimental procedure

Various "classic" LPS systems with solid–liquid density differences ranging from 0–9 g cm^{-3} were selected for this study. Table I shows the alloy compositions and solid–liquid density differences. The density differences were empirically determined at the solidus temperature using the inverse rule of mixtures while accounting for the density decrease associated with heating and the solubility between the two phases. The target experimental compositions were estimated using the calculated densities and the volume fraction from the lever rule. A constant solid volume fraction of 0.3 was used in the calculations for all systems. A more detailed description of these calculations is presented elsewhere [9]. Note that the Fe–Cu system is anomalous in that the liquid is more dense than the solid. The powders were mixed for 30 min using a turbula mixer and cold isostatically compacted at 140 MPa into cylindrical compacts with approximately 10 mm diameter and 20 mm height. These compacts were presintered to reduce oxides and sintered at pre-designated temperatures. Table II lists the processing parameters for the various systems. Sintering was performed in alumina crucibles with inner dimensions slightly larger than the compacts, because the large

0022–2461 © *1995 Chapman & Hall*

liquid-volume fraction present at the sintering temperatures used in this study promoted considerable slumping and distortion. A heating rate of $10\,^{\circ}C\,min^{-1}$ was used between room temperature and the presinter temperature and also between the presinter temperature and the sintering temperature. All samples were furnace cooled from the sintering temperature.

The sintered samples were cross-sectioned and mounted for metallographic analysis. The solid-volume fraction and height of the settled region were measured. Photomicrographs were taken and used to analyse the microstructure. To avoid frictional wall effects, all photomicrographs were taken at the centre of the samples. The solid-volume fraction was measured using image analysis programs on a personal computer. Over 200 grains per sample were measured. The height of the liquid- and solid-settled regions were measured to two significant figures directly from each sample using a digital caliper.

3. Results

A solid–liquid density difference, ($\Delta\rho$), in a 0.3 solid-volume fraction liquid-phase sintering case, causes segregation between the solid and liquid phases. The grains settle to the bottom of the specimen when the density of the solid phase is greater than that of the liquid phase. Floating occurs when the solid-phase density is less than that of the liquid phase. Suspension is observed when no density difference exists between the solid and the liquid phase. An example of solid and liquid segregation is shown in Fig. 1 for a W–Ni compact sintered at 1500 °C for 1 h in hydrogen. In this system the solid-phase density is greater than the liquid-phase density and the solids settle at the bottom. The settled region is rounded on the top because the matrix migrates to the outer region of the compact at a faster rate than the solid phase upon melting.

The height of the settled region is dependent on the alloy, its composition, the sintering temperature, and the solid–liquid density difference. This is illustrated graphically in Fig. 2 by plotting the normalized height, h/h_0, of the samples versus the solid–liquid density difference. The normalized height is defined as the height of the segregated solid region, h, divided by the total height of the sample, h_0. The normalized height of the settled solid region decreases as the density difference increases. It decreases rapidly at low

TABLE I Alloy compositions and calculated density differences

Alloy composition (wt %)	$\rho_s - \rho_l$ ($g\,cm^{-3}$)	
	−	+
28Co–72Cu	0.0	
82.9Nb–8.7Ni–8.4Fe		0.1
28Fe–72Cu	0.8	
65.5Mo–34.5Ni		1.0
27TiC–73Ni		3.3
69W–31Ni		7.8
60W–28Ni–12Fe		9.0

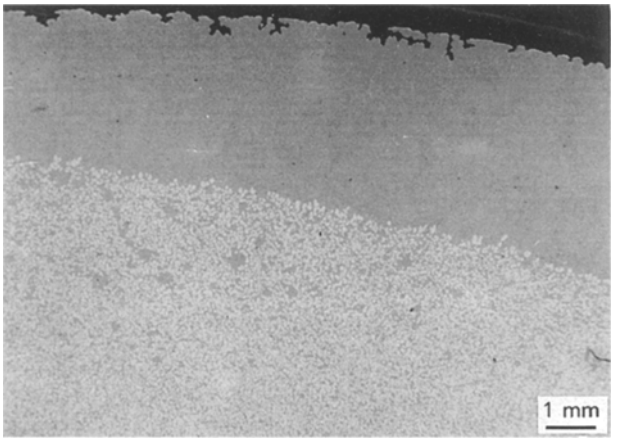

Figure 1 Scanning electron micrograph of the cross-section of 0.3 solid-volume fraction W–Ni system where the solid density is greater than the liquid-phase density. The centre of the specimen is on the left side of this cross-section while the outer edge of the specimen is on the right.

density differences, then reaches a minimum at a density difference of $9\,g\,cm^{-3}$. The rapid decrease in settled region height with an increase in solid–liquid density difference at low density differences, signifies that slight density differences offer enough driving force for settling.

Gradients in microstructure were observed in the settled region for systems where settling occurred. Fig. 3 shows scanning electron micrographs of the top and bottom of the settled region for three different density-difference systems. Fig. 3a and b show the top and bottom regions, respectively, of a Cu–Co system. The cobalt grains in the Cu–Co system ($\Delta\rho = 0\,g\,cm^{-3}$) were suspended in the matrix and no gradients in microstructure were present. The bottom of the Mo–Ni settled region had a greater

TABLE II Experimental processing parameters of the various alloy systems

Composition (wt %)	Presinter temp (°C)	Presinter time (min)	Presinter atm.	Sinter temp. (°C)	Sinter time (min)	Sinter atm.
60W–28Ni–12Fe	800	60	H_2	1500	60	H_2
82.9Nb–8.7Ni–8.4Fe	800	60	Vac.	1400	60	Vac
72Cu–28Fe	1000	60	H_2	1200	30	Ar
69W–31Ni	800	60	H_2	1550	60	H_2
73Ni–27TiC	800	60	H_2	1400	120	H_2
72Cu–28Co	1000	60	H_2	1150	60	Ar
65.5Mo–34.5Ni	800	60	H_2	1500	60	H_2

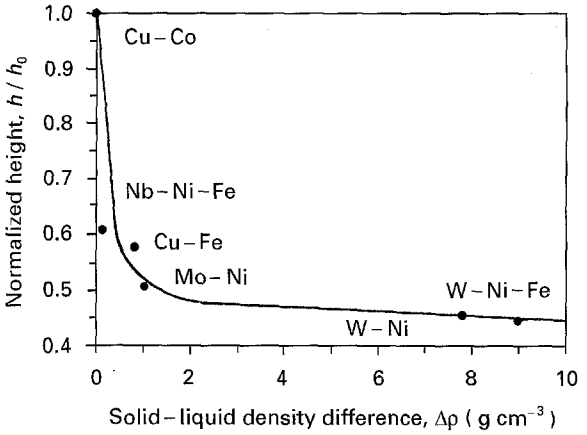

Figure 2 Dependence of the solid-segregated region height on solid–liquid density difference. The normalized height is defined as the height of the solid-segregated region divided by the total height of the sample.

solid-volume fraction than the top (Fig. 3c and d). This same trend was also observed in the W–Ni (Fig. 3e and f) and W–Ni–Fe systems. Kipphut *et al.* [5] previously reported that besides volume fraction of solid, there were also grain-size, contiguity and connectivity gradients aligned with the gravitational gradients. Similar gradients were found in these samples. The solid-volume fraction at the top and bottom of the settled region versus the density difference are plotted in Fig. 4. The solid-volume fraction in the settled region increases with density difference. Also, the difference between the top volume fraction and the bottom volume fraction becomes greater as the density difference increases.

The solid-volume fraction is shown in Fig. 5 as a function of normalized height, h/h_0, for the different systems. The h parameter was measured at 1 mm intervals from the bottom to the top of the settled region. The volume fraction is linearly dependent on

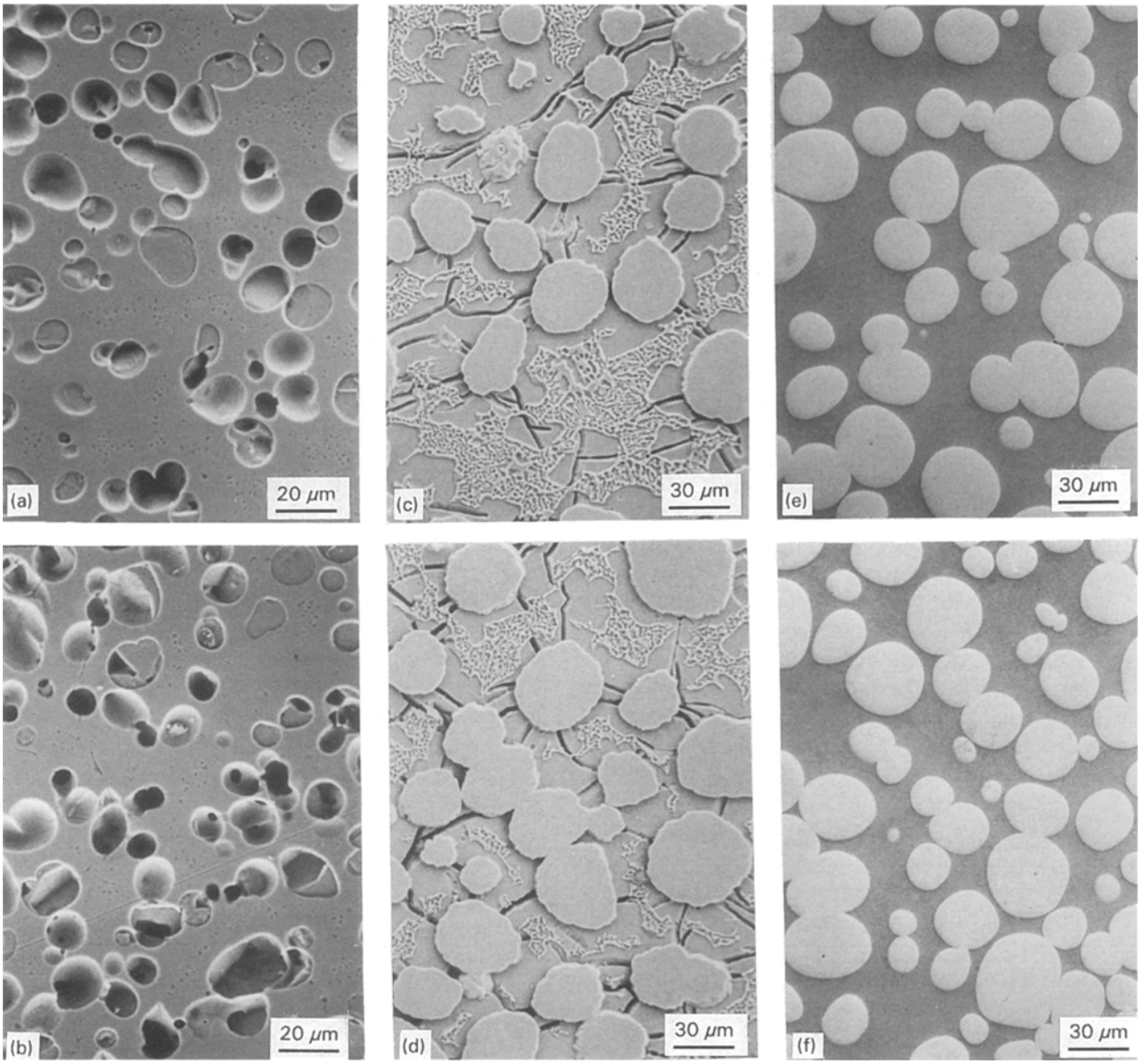

Figure 3 Scanning electron micrographs of the top and bottom region of a Co–Cu system ($\Delta\rho = 0\,g\,cm^{-3}$), a Mo–Ni system ($\Delta\rho = 1.0\,g\,cm^{-3}$), and a W–Ni system ($\Delta\rho = 7.8\,g\,cm^{-3}$): (a) Co–Cu top, (b) Co–Cu bottom, (c) Mo–Ni top, (d) Mo–Ni bottom, (e) W–Ni top, (f) W–Ni bottom.

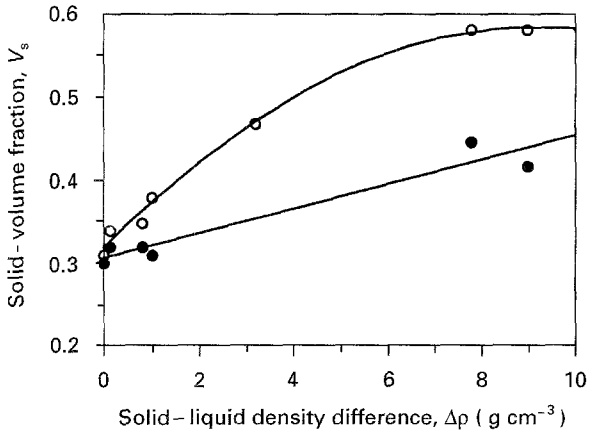

Figure 4 The solid-volume fraction at the top and bottom of the settled region versus the solid–liquid density difference. (○) Data at the completely settled region, (●) data at last settled region.

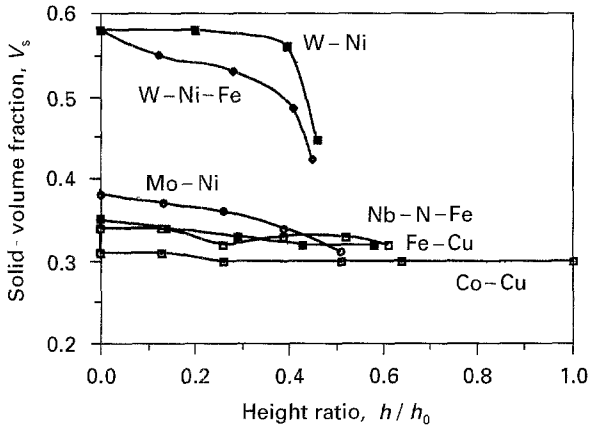

Figure 5 The solid-volume fraction as a function of height ratio for a range of density difference systems. h was measured at 1 mm intervals from the bottom to the top of the settled region and h_0 is the total height of the sample.

vertical position at low density differences and becomes non-linear as the density difference increases.

4. Discussion

The solid-volume fraction in the completely settled region is limited by the formation of a solid-phase skeleton. The limiting mechanism is related to the solid–liquid density difference. If the density difference is sufficiently large, then the solid-volume fraction approaches a value of 0.60 in the settled region, which is similar to the packing obtained for randomly stacked monosized spheres under 1 g in air. A high density difference is believed to cause the settling of discrete grains and a deflocculated structure and thus, a packing volume similar to that of non-interacting spheres. From this observation, one may hypothesize that a critical density difference exists above which the settled solid-phase volume fraction is independent of the density difference between the phases. Slight variations in solid-volume fraction may exist above this critical density difference due to kinetic and thermodynamic concerns, such as Ostwald ripening and wetting of the solid phase, respectively. As the density difference decreases, the velocity of the settling grains decreases, which allows time for neck growth between grains. This produces a flocculated structure, thereby retarding grain packing and resulting in a less densely packed microstructure. The grains may actually bond prior to complete settling and produce chain-like clusters which do not pack as well as discrete grains. It is recognized that agglomerated structures do not pack as well as discrete particles [10]. In the case where no density difference exists between the solid and liquid phase, the grains remain suspended which is similar to the behaviour observed in the microgravity experiment [11–14] where no gravity-induced settling occurs.

5. Conclusions

Liquid-phase sintering of dilute (0.3 volume fraction solid) systems produces microstructures dominated by the solid–liquid density difference. Three different significant solid–liquid density differences exist – greater than zero, less than zero, and equal to zero. A density difference greater than zero (solid-phase density greater than liquid-phase density) causes the solid grains to settle in the liquid phase. A density difference less than zero (solid-phase density less than liquid-phase density) causes the solid grains to float in the liquid phase. A density difference equal to zero allows the solid grains to remain suspended in the liquid phase.

Microstructural gradients exist along the direction of gravity within the settled region. The largest solid-volume fraction was predominantly observed at the bottom of the settled region. The difference in microstructural parameters between the top and bottom became larger as the density difference increased. The exact reason for this is unclear – coalescence is believed to be easier in the less densely packed lower density difference cases. Yang and German [4] have shown that the difference between the solid-volume fraction at the top of the settled region and at the bottom of the settled region decreases with increased sintering times for a low solid-volume fraction LPS W–Ni–Fe system. This suggests that either grain packing becomes complete with increase in sintering time, or that coarsening kinetics at the bottom of the settled region slow down due to a decrease in solid–liquid interfacial area which allows the coarsening at the top of the settled region to "catch up" with that of the bottom.

Acknowledgements

The authors thank NASA for supporting this research under the direction of G. Santoro and R. DeWitt for the Lewis Research Center, Cleveland, OH.

References

1. S. C. HARDY and P. W. VOORHEES, *Metall. Trans.* **19A** (1988) 2713.
2. C. M. KIPPHUT, R. M. GERMAN, A. BOSE and T. KISHI, "Advances in Powder Metallurgy", Vol. 2, in Proceedings of

the 1989 Powder Metallurgy Conference and Exhibition, edited by T. G. Gasbarre and W. F. Jandeska (Metal Powder Industries Federation, Princeton, NJ, 1989) p. 415.
3. C. M. KIPPHUT, T. KISHI, A. BOSE and R. M. GERMAN, "Progress in Powder Metallurgy", Vol. 43, in Proceedings of the 1987 Annual Powder Metallurgy Conference, edited by C. L. Freeby and H. Hjort (Metal Powder Industries Federation, Princeton, NJ, 1987) p. 93.
4. S. C. YANG and R. M. GERMAN, *Metall. Trans.* **22A** (1991) 786.
5. C. M. KIPPHUT, A. BOSE, S. FAROOQ and R. M. GERMAN, *ibid.* **19A** (1988) 1905.
6. A. N. NIEMI and T. H. COURTNEY, *Acta Metall.* **31** (1983) 1393.
7. S. S. KANG and D. N. YOON, *Metall. Trans.* **13A** (1982) 1405.
8. Z. FANG and B. R. PATTERSON, "Modern Developments in Powder Metallurgy", Vol. 18, in Proceedings of the 1988 International Powder Metallurgy Conference, edited by P. U. Gummeson and D. A. Gustafson (Metal Powder Industries Federation, Princeton, NJ, 1988) p. 615.
9. D. F. HEANEY, Master's Thesis, (Pennsylvania State University, University Park, PA, (1993) pp. 16–18.
10. R. M. GERMAN, in "Particle packing characteristics" (MPIF, Princeton, NJ, 1989) p. 59.
11. L. B. EKBOM and A. ELIASSON, "Modern Developments in Powder Metallurgy", Vol. 19, in Proceedings of the 1988 International Powder Metallurgy Conference, edited by P. U. Gummeson and D. A. Gustafson (Metal Powder Industries Federation, Princeton, NJ, 1988) p. 63.
12. L. B. EKBOM, *Int. J. Refract. Met. Hard Mater.* **6** (1987) 231.
13. L. B. EKBOM and A. ELIASSON, *Adv. Space Res.* **8** (1988) 315.
14. L. B. EKBOM, H. FREDRILSSON and A. ELIASSON, *High. Temp. High Press.* **21** (1989) 507.

Received 25 January 1994
and accepted 7 June 1995